Smart Indentation Methods: The Application of Neural Networks

Priv.-Doz. Dr.-Ing. Norbert Huber and Dipl.-Ing. Edouard Tioulioukovski
Forschungszentrum Karlsruhe, Institut für Materialforschung II
Postfach 3640, 76021 Karlsruhe, Germany

Abstract

In the last decade, the nanoindentation technique has become one of the most important characterization methods in micro dimensions. The experimental and analytical techniques have been pushed towards an identification method that can compete with tensile tests. It is self-evident to apply these powerful tools in macro dimensions as well, where the nanoindentation technique has its roots. In this paper a new method is presented how the true stress-strain curve as well as the viscosity and creep behaviour of a given material can be extracted from the indentation curve by using a smart analysis tool based on neural networks. Finite Element simulations are carried out for randomly chosen sets of material parameters and maximum indentation depth. The resulting load-depth and depth-time curves are collected in a database together with the material parameters. With this database neural networks are trained to identify the material parameters from measured load-depth and depth-time curves.

1. Introduction

The conventional hardness test is well known to characterize the mechanical properties of materials. The advantages include that only small amounts of material are needed. Because of its non-destructive nature the experiment is multi repeatable with the same specimen.
Tabor [1] and Atkins and Tabor [2] have shown that either a spherical indenter or several pyramidal indenters with different tip angles have to be used, when the stress-strain relation of a bulk material is to be investigated. For example, one can determine the Young's modulus (see e.g. [1,3-6]), the hardening behaviour according to monotonic loading [1,5,7,8], viscosity effects [9,10] and the parameters governing the response of nonlinear isotropic and kinematic hardening of Armstrong-Frederick type [11,12].
The proposed method solves the inverse mechanical problem, i.e. the identification of viscoplastic material parameters, using neural networks and the Finite Element method. In order to gain the same amount of information on the mechanical behaviour from conventional tensile experiments, a series of experiments as tension at different strain rates and relaxation experiments are needed.
To avoid a tip change we restrict our work to spherical indenters. All material parameters are obtained from one experiment. The complex inverse function is approximated by a neural network which is trained using data from randomly distributed Finite Element simulations.

2. Spherical indentation

The indentation technique is further developed from microhardness testing and requires a continuous load and depth measurement. In what follows, t, h and P denote time, penetration depth and load on the indenter, respectively, as displayed in Fig. 1.
When a spherical indenter with radius R penetrates a viscoplastic homogeneous material, the measured load-depth response is determined by the load rate $\dot{P}$ and the material properties. As already found by Tabor, a good estimate of the stress-strain relation can be determined from indentation experiments by using the relations

$$\sigma = P_m / 2.8, \tag{1}$$

$$\varepsilon = 0.2a / R, \tag{2}$$

where a denotes the contact radius of the impression and $P_m = P/(\pi a^2)$ defines the mean pressure in the contact region.

Since most microindentation devices work load controlled a creep process ($P = const$) is inserted at the maximum load for duration T in order to gain information about the viscous properties and the equilibrium state. Another possibility would be a relaxation process with $h = const$, which is not considered here.

The time, depth and load at the end of the loading process is denoted by t_0, h_0 and P_0, respectively. The corresponding quantities at the end of the creep process are denoted by t_t, h_t and $P_t = P_0$, respectively. The unloading stiffness S is defined by $S := dP/dh|_{h=h_t}$ from which the reduced modulus $E_r = E/(1-\nu^2)$ can be determined.

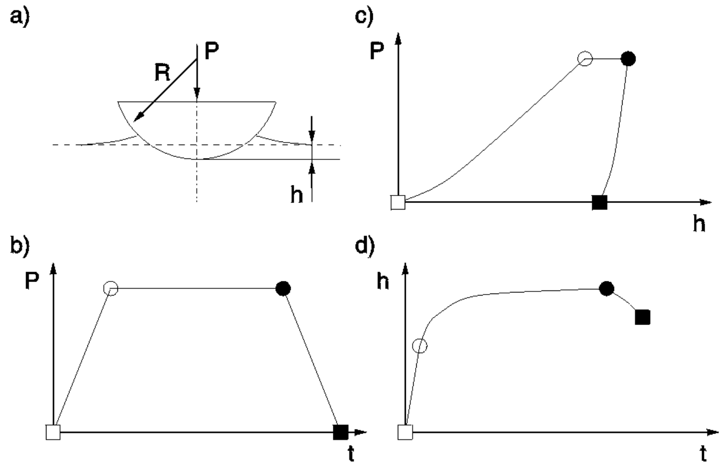

Fig. 1: (a) Geometry of spherical indentation; (b) Load-time history; (c) Load-depth curve; (d) Depth-time response

3. Computational methods

3.1 Constitutive model

The viscoplasticity model used is formulated for finite deformations and satisfies the second law for any admissible process. It has been implemented in ABAQUS as a so-called UMAT subroutine. For details respecting the constitutive equations see [14,15]. In what follows, we consider a simplified case of viscoplasticity with nonlinear isotropic hardening. The material parameters E and ν denote the Young's modulus and Poisson's ratio, respectively.

The evolution equation for the accumulated plastic strain rate $\dot{s} := |\dot{\varepsilon}_p|$ is

$$\dot{s} = \langle F \rangle^m / \eta, \tag{3}$$

where m and η are viscosity parameters. In addition, the isotropic hardening rule for the isotropic hardening variable k

$$\dot{k} = (\gamma - \beta(k - k_0))\dot{s} \tag{4}$$

is determined by three hardening parameters: the yield stress k_0, the initial work hardening rate γ and an additional parameter β that limits the maximum isotropic hardening to

$k_\infty = k_0 + \gamma / \beta$. For a constant plastic strain rate $\dot{\varepsilon}_p > 0$, we obtain an overstress $F = (\eta \dot{\varepsilon}_p)^{1/m}$ and the ultimate tensile strength is $R_m = k_\infty + F$.

3.2 Finite Element simulations

The direct problem of calculating the depth-time behaviour $h(t)$ for a given load-time history $P(t)$ is solved numerically using the Finite Element method (for details see e.g. [16]). The input quantities are the material parameters E, ν, k_0, γ, β, η, m, the indenter radius R, the load rate $\dot{P}$, the maximum load P_0, and the creep time T.
The Finite Element mesh is of unit size while the indenter radius is $R = 0.1mm$ so that the contact area is about less than 5 percent of the mesh size. The Finite Element mesh consists of quadriliteral axisymmetric eight-node elements and is refined in the contact area sufficiently to ensure a good quality for the loading response. The indenter is assumed to be rigid and no friction is present between the indenter and the specimen surface.

3.3 Neural networks

Artificial neural networks represent a qualified tool for solving complex inverse problems in computational mechanics. An overview about some relevant applications is given in [17,18]. Neural networks are flexible functions $\vec{y} = f(\vec{x}, \overline{w})$ which map an input vector $\vec{x}$ to an output vector $\vec{y}$. The network is defined by the number of neurons and layers (see Fig. 2) and the values of the synaptic weights $\overline{w}$, which are indicated by arrows in Fig. 2. The data for the training consist of pairs of desired function values (outputs $\vec{d}$) for corresponding inputs $\vec{x}$. Using a backpropagation algorithm (see e.g. [19]), the error between the outputs and the desired values $E = \sum (y_l(x_i, w_{ij}) - d_l)^2$ is minimized and the synaptic weights are adjusted. In this way, the network can be trained to represent any unique relation given by a number of examples.
In the case of parameter identification the inputs are defined by the load-depth and depth-time response while the desired outputs are the material parameters of our model. Neural networks are of approximative nature. In order to achieve accurate results experience is necessary for the formulation of proper input and output definitions [17]. For more details about feed forward neural networks, data preparation and training algorithms see [17,19].

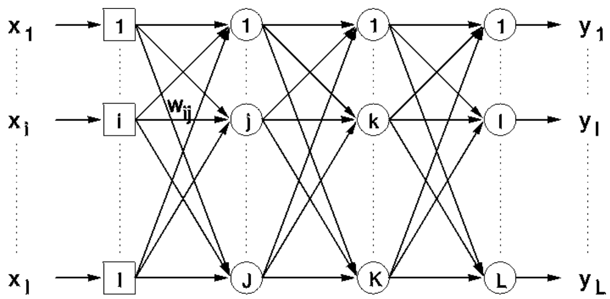

Fig. 2: Example of a feed forward neural network with four layers

4. Identification of material parameters

In general, two possibilities exist for the identification of material parameters from inhomogeneous experiments. The commonly used method is to perform Finite Element simulations starting from an assumed set of material parameters and to optimize the material parameters by minimizing the square error of the difference between the numerical and the experimental data. This method has the advantage, that its result is the best fit for the assumed constitutive model and the performed experiment. However, it is uncertain if the set of material parameters, obtained, is unique. In addition, for a second experiment all simulations of the prior identification are useless and the whole number of Finite Element simulations is needed again.

In this work, the inverse problem is solved by neural networks. A number of Finite Element simulations of the spherical indentation test are performed by randomly chosen sets of material parameters and indentation depth h_0. The limits for the material parameters are chosen in a wide range so that the prospective materials can be identified. The value of h_0 is allowed to be within a wide range of $0.01 \le h_0 / R \le 0.15$. On the basis of the obtained numerical load-depth and creep responses the relation between the measurable data and the underlying material parameters is trained to the neural network, as illustrated in Sect. 3.3. If the problem is non-unique, the neural network will not be able to solve the inverse problem, indicated by a high output error at the concerned output neuron. In the majority of cases it is possible to modify the loading history, e.g. by inserting of creep or unloading phases and choosing the right geometry or depth range, in order to provide the relevant information, needed.

Another important point, which is relevant for the identification accuracy, is the choice of the input and output definitions. Dimensionless quantities should be preferred to make the network as general as possible. Reducing the number of input neurons to a minimum prevents big network structures, which tend to classify. In what follows, the input quantities are defined for the neural network. Equation (5) composes information with respect to the ratio of the average contact radius rates for loading and creep. Equations (6)-(8) and (9)-(11) represent the shape of the loading response and the creep curve, respectively. The unloading stiffness is provided by (12). Note, that the index 0 and t denote the begin and the end of creep, respectively.

$$x_1 := \dot{a}_0 / \dot{a}_{cr} \tag{5}$$

$$x_2 := h(0.25t_0) / h_0 \tag{6}$$

$$x_3 := h(0.5t_0) / h_0 \tag{7}$$

$$x_4 := h_0 / R \tag{8}$$

$$x_5 := (h(t_0 + 0.05T) - h_0) / h_0 \tag{9}$$

$$x_6 := (h(t_0 + 0.1T) - h_0) / h_0 \tag{10}$$

$$x_7 := (h(t_0 + T) - h_0) / h_0 \tag{11}$$

$$x_8 := Sh_t / P_t \tag{12}$$

The output quantities of the neural network consist of material parameters, which are made dimensionless by estimates including a priori knowledge. This has, in addition to the non-dimensional formulation, the advantage that the neural network is only responsible for determining the correction factor to the estimate. Using this method, neural networks can yield a comparable high accuracy [17]. The following equations use prior knowledge from determining the Young’s modulus [7]

$$y_1 := E_r \sqrt{Rh_t} / S \, , \tag{13}$$

the Tabor relation (1)

$$y_2 := k_0 / P_{m0}, \tag{14}$$

$$y_3 := \gamma / P_{m0}, \tag{15}$$

$$y_4 := R_m / P_{m0}, \tag{16}$$

$$y_5 := F' / (P_{m0} - P_{mt}), \tag{17}$$

and the form of the evolution equation for the overstress from the constitutive model combined with Tabor's equation for the plastic strain (2)

$$y_6 := \left(\dot{a}_{cr} / \dot{a}_0\right)^{1/m}. \tag{18}$$

In (5)-(18) the average contact radius rates and mean pressures are given by $\dot{a}_0 := \sqrt{2Rh_0} / t_0$, $\dot{a}_{cr} := \sqrt{2R(h_t - h_0)} / (t_t - t_0)$, and $P_{m0} := P_0 / (2\pi R h_0)$, $P_{mt} := P_t / (2\pi R h_t)$, respectively. Inserting (2) in (3), the global indentation overstress F' is given by the relation $F' := (0.2\eta \dot{a}_0 / R)^{1/m}$. When the values of y_1 to y_6 are determined by the neural network, the system of equations (13)-(18) can be solved with respect to the material parameters. As usual, the reduced modulus $E_r = E / (1 - \nu^2)$ is determined, where the Poisson's ratio ν is assumed to be $\nu = 0.3$ for all Finite Element simulations.

The neural network consists of four layers with 8, 20, 10 and 6 neurons, respectively, and is trained 5000 epochs with 145 patterns. It has been verified by additional patterns that were not included in the training. The accuracy of the validation patterns is comparable to that of the training patterns and the network provides a good generalization.

The trained neural network was applied to experimentally measured curves displayed in Fig. 3(a). The indentation experiments are carried out using an Ultra-micro Indentation System UMIS 2000 with a spherical indenter of $R = 10\mu m$. The material parameters identified from the experimental data yield the stress-strain curves displayed in Fig. 3(b). The simulation of the tensile experiment consists of strain controlled loading with $\dot{\varepsilon} = 10^{-4}$ and inserted relaxation phases of $1000s$ in order to visualize the contribution of the viscous overstress. In contrast to the observed creep behaviour during the indentation experiment the viscous part is most significant for the ferritic steel.

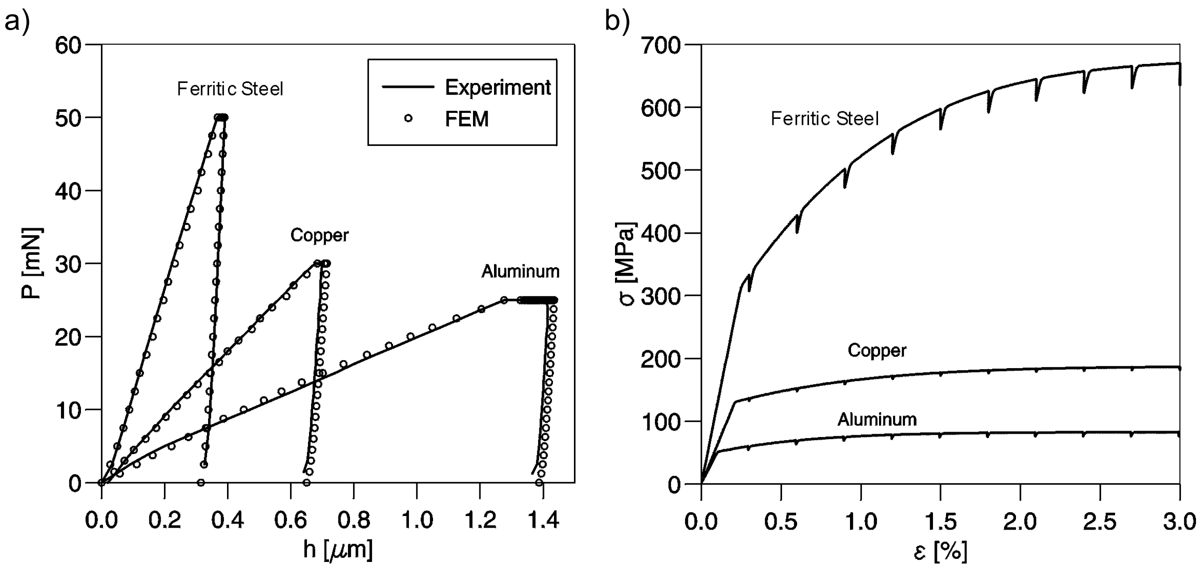

Fig. 3: (a) Experimental measured load-depth curves; (b) identified stress-strain responses

For a first verification, a simulation of the indentation experiment was carried out using the identified material parameters (no optimization was carried out). The predictions of the numerical simulations are in excellent agreement with the experimental curves for all parts of the experiment: the loading creep and unloading process. It is worth to mention, that the viscous part in the constitutive model does not only produce creep at constant load. Furthermore, it is responsible for a steep rise at the very beginning of the loading response. This effect is very pronounced for aluminium as it can be seen in Fig. 3(a) and cannot be observed from simulations with plasticity models (see e.g. [11,12]).

Conclusions

The present paper has shown that the indentation experiment has a giant potential in determination of more than just hardness. It has been demonstrated for a viscoplasticity model how the material parameters of the hardening response, the viscosity parameters and the Young's modulus can be identified. Extensions towards the identification of kinematic hardening, static recovery as well as thin films or hardened layers are possible in the same manner. The proposed smart indentation method distinguishes itself by combining the advantages of an innovative constitutive model, a loading history that allows a unique identification of the material parameters, the numerical solution of the inelastic contact problem by the Finite Element method and the application of neural networks for an explicit solution of the inverse problem. Having the trained neural network, no more Finite Element simulations are needed and the identification can be carried out within some milliseconds.

Acknowledgments

The financial support by the Deutsche Forschungsgemeinschaft (DFG) is gratefully acknowledged.

References

1. D. Tabor, Hardness of Metals, University Press, Cambridge, 1951.
2. A.G. Atkins, D.T. Tabor, J. Mech. Phys. Solids 13 (1965) 149.
3. M.F. Doerner, W.D. Nix, J. Mater. Res. 1 (1986) 601.
4. G.M. Pharr, W.C. Oliver, F. R. Brotzen, J. Mater. Res. 7 (1992) 613.
5. J.S. Field, M.V. Swain, J. Mater. Res. 8 (1993) 297.
6. N. Huber, D. Munz, Ch. Tsakmakis, J. Mater. Res. 12 (1997) 2459.
7. E. Meyer, Zeits. Ver. Dt. Ing., 52 (1908) 82.
8. S. Jayaraman et al., Int. J. Solids Structures 35 (1998) 365.
9. M.J. Mayo, W.D. Nix, Acta Metall. 36 (1988) 2183.
10. V. Raman, R. Berriche, J. Mater. Res. 7 (1992) 627.
11. N. Huber, Ch. Tsakmakis, J. Mech. Phys. Solids. 47 (1999) 1569.
12. N. Huber, Ch. Tsakmakis, J. Mech. Phys. Solids. 47 (1999) 1589.
13. N. Huber, Ch. Tsakmakis in B. Michel and T. Winkler (Eds.), Micro Materials, Berlin, 1997, p. 188.
14. E. Diegele, W. Jansohn, Ch. Tsakmakis, Comput. Mech. 25 (2000) 1.
15. E. Diegele, St. Hartmann, Ch. Tsakmakis, Comput. Mech. 25 (2000) 13.
16. N. Huber, Ch. Tsakmakis, J. Eng. Mat. Tech. 120 (1998) 143.
17. N. Huber, Application of neural networks to nonlinear problems of mechanics, Habilitation thesis, in german, FZKA-Report 6504, Forschungszentrum Karlsruhe (2000).
18. G. Yagawa, H. Okuda, Model. Simul. Mat. Sci. Engrg. 3 (1996) 435.
19. S. Haykin, Neural Networks - A Comprehensive Foundation, Macmillan, New York, 1994.